out that the splitting of the metal d orbitals is primarily due to a crystal-field effect (the asymmetric crystal field term $C_2{}^0$), rather than to any significant metal–ligand bonding involving the d's.

(23) L. Pauling, "The Nature of the Chemical Bond", Cornell University Press, Ithaca, N.Y., 1960, p 172.
(24) A. L. Allred and E. G. Rochow, *J. Inorg. Nucl. Chem.*, **5**, 764 (1958), and later papers.
(25) H. Gilman and R. E. Brown, *Recl. Trav. Chim. Pays-Bas*, **48**, 1133 (1929).
(26) All atomic orbital energies were calculated by Topiol (ref 7) using essentially the same basis sets employed here. These results agree closely with atomic Hartree–Fock values.
(27) E. G. Rochow, R. T. Hurd, and R. M. Lewis, "The Chemistry of Organometallic Compounds", Wiley, New York, N.Y., 1957, p 83.
(28) Reference 27, p 78.
(29) N. B. Hannay and C. P. Smyth, *J. Am. Chem. Soc.*, **68**, 171 (1946).
(30) R. G. Pearson, *J. Am. Chem. Soc.*, **85**, 3533 (1963); *Science*, **151**, 172 (1966). A compendium of work on this subject is R. G. Pearson, Ed., "Hard and Soft Acids and Bases", Dowden, Hutchinson and Ross, Stroudsburg, Pa., 1973.
(31) S. Ahrland, J. Chatt, and N. R. Davies, *Q. Rev., Chem. Soc.*, **12**, 265 (1958).
(32) Similar conclusions (that larger electronegativity distances result in shorter bonds) come from the Schomaker–Stevenson relation (cf. Ref 23, p 229).
(33) R. G. Pearson, *J. Chem. Educ.*, **45**, 643 (1968).
(34) J. B. Collins, P. R. Schleyer, J. S. Binkley, and J. A. Pople, *J. Chem. Phys.*, **64**, 5142 (1976).
(35) A. J. H. Wachters, *J. Chem. Phys.*, **52**, 1033 (1970).
(36) T. H. Dunning, personal communication.

The Shapes and Other Properties of Non-Transition Element Complexes. 1. AB6

Benjamin M. Gimarc,*[1a] Joel F. Liebman,*[1b] and Michael Kohn[1a]

Contribution from the Department of Chemistry, University of South Carolina, Columbia, South Carolina 29208, and Department of Chemistry, University of Maryland, Baltimore County, Baltimore, Maryland 21228. Received December 1, 1976

Abstract: Qualitative MO methods are used to study the properties of six-coordinate complexes of the main group elements of the periodic table. The hexahalides are emphasized. The simplest possible AO basis set is used to form MOs. No d orbitals are considered. MO correlation diagrams are presented to compare energies of AB_6 complexes in octahedral (O_h) and trigonal prismatic (D_{3h}) geometries. The O_h and D_{3h} conformations possible for AB_6 complexes are compared to the staggered and eclipsed conformations of ethane. The qualitative MO model predicts that 12-electron complexes ($PF_6{}^-$, SF_6, $ClF_6{}^+$, for example) should be rigidly octahedral but the 14-electron complexes (XeF_6 and isoelectronic species) should be considerably less rigidly octahedral. For the 14-electron series there should be a trend of increasing ease of distortion from octahedral shape with decreasing difference in electronegativity between the central atom and the ligands. No ten-electron complexes are known. The qualitative model predicts these to be open-shell cases and octahedral. Complexes with six and eight electrons should be trigonal prismatic. Reported examples are $LiH_6{}^+$ and $BF_2H_4{}^+$. MO correlation diagrams describe the dissociation of AB_6 complexes into $AB_4 + B_2$. Qualitative MO arguments are used to explain the differences in bond lengths and strengths between 12- and 14-electron complexes and to rationalize trends in complex stabilities as related to ligand substitution.

Introduction

Our object in this paper is to explain, rationalize, or predict as many of the properties of selected AB_6 complexes as possible using qualitative arguments within the framework of molecular orbital (MO) theory and relying on a single well-defined model that can be applied to other classes of complexes. Many of the properties discussed here have already been explained, perhaps even more simply, by using a diverse set of models. The point here is unity. One justification for this is aesthetics: it is pleasing to have a single model that explains a large number of facts and MO theory does provide a well-defined connection between the qualitative concepts and the basic laws of physics that underlie chemistry. A more practical reason is that MO theory is the most successful and convenient method for the quantitative application of quantum mechanics to chemistry. Therefore, a powerful computative method exists for testing the arguments and conclusions of the qualitative MO model. Such checks are not always possible or convenient for other qualitative models.

For the complexes to be considered here, the central atom A will be one of the main group elements of the periodic table. To limit our study further we will consider only those complexes in which the ligands B are individual atoms. In most cases the ligands are halogens, although a few oxides are known. We will also mention some real and hypothetical examples which involve hydrogen ligands. We omit transition metal complexes in order to avoid discussion and representation of d atomic orbitals, although similar arguments could be

applied to them. We will compare octahedral (O_h) and trigonal prismatic (D_{3h}) structures. In a recent paper Hoffmann, Howell, and Rossi[3] have used extended Hückel calculations and qualitative MO arguments to rationalize the preference of most AB_6 complexes for octahedral geometry. They also consider a bicapped tetrahedral structure. Hoffmann, Howell, and Rossi have studied the transition metal complexes and the effect of d atomic orbitals, topics we have ignored. Besides the 12-valence electron complexes of the main group elements reviewed by Hoffmann and co-workers, we consider structures for 6-, 8-, 10-, and 14-electron complexes. We also discuss other properties including dissociation mechanisms, bond lengths and strengths, and relative stabilities of AB_6 complexes. Urch has also published an important qualitative study of the relative stabilities of non-transition element AB_6 complexes.[4]

Many of the rules of qualitative MO theory have already been discussed elsewhere,[2] but in this and subsequent papers we will use additional arguments which we present here. The qualitative MO model follows the formalism of the extended Hückel method.[5] The MOs ϕ_k are formed by linear combinations of normalized atomic orbitals (AOs) χ_r: $\phi_k = \sum_r c_{rk}\chi_r$. The MOs must be normalized:

$$\langle \phi_k^2 \rangle = \sum_r c_{rk}^2 + 2 \sum_{r<s} c_{rk}c_{sk}S_{rs} = 1 \qquad (1)$$

where S_{rs} is the overlap between AOs χ_r and χ_s. The total energy E of a molecule is the sum of the energies ϵ_k of occupied MOs: $E = \sum \epsilon_k$, where the summation is over the valence electrons. The orbital energy ϵ_k can be calculated as $\epsilon_k =$

$\langle \phi_k/\mathcal{H}(1)/\phi_k \rangle$, where $\mathcal{H}(1)$ is a one-electron Hamiltonian operator that includes the effect of electron–electron repulsions in an average way. Assuming that the off-diagonal matrix elements $H_{rs} = \langle \chi_r/\mathcal{H}(1)/\chi_s \rangle$ are directly proportional to the overlap S_{rs}, the orbital energy ϵ_k can be written as[6]

$$\epsilon_k = \sum_r c_{rk}^2 H_{rr} + K \sum_{r \neq s} c_{rk} c_{sk} S_{rs}$$

If the coefficients c_{rk} and c_{sk} do not change much during variations in angular geometry (although they often do), we can express the changes $\Delta \epsilon_k$ in orbital energies as

$$\Delta \epsilon_k \propto \sum_{r \neq s} c_{rk} c_{sk} \Delta S_{rs} \qquad (2)$$

Equation 2 says that MO energy changes will be large if the overlap changes ΔS_{rs} are large or if the coefficients $c_{rk} c_{sk}$ are large or if there are many accumulating terms in the summation. Changes in AO overlap can be estimated pictorially, the number of overlapping AO pairs can be counted, AO phase relationships can be deduced from orbital symmetry, and the relative magnitudes of the AO coefficients can be inferred qualitatively.

The magnitudes of the coefficients are determined in part by MO normalization. Suppose all the AOs enter a MO with the same phase and that all overlaps are positive as they usually are. Then the individual coefficients must be small in order that the sum of squares of coefficients plus cross terms times overlaps all add up to unity in eq 1. If there are phase differences among the AOs, then some cross terms will be negative and the squared terms, and therefore the coefficients themselves, will have to be larger so that the summation still adds up to unity. In general, the higher the energy of a MO, the more nodes or phase differences there will be between component AOs and the larger the AO coefficients will be, producing larger $\Delta \epsilon_k$ from eq 2. Large $\Delta \epsilon_k$ and large coefficients determine molecular shapes and other properties. Therefore, MO normalization, eq 1, and the orbital energy proportionality, eq 2, justify the well-known rule that the highest occupied MO often determines molecular properties.

MO orthogonalization also plays a part in determining the relative sizes of AO coefficients by establishing a balance between various regions of different phase within the MO.

It is easiest to compose MOs for the structure of highest symmetry which severely limits the kinds and combinations of AOs that can enter a particular MO. Orbitals for less symmetric shapes can then be generated by angular deformations of the MOs for high symmetry. In some cases the lower symmetry MOs so produced may not contain the full complement of AOs allowed by the lower symmetry. One way to adjust such deficient MOs is by mixing pairs of MOs of the same symmetry classification. Mixing is more important the higher the energy of the MO. We can satisfactorily account for mixing in the higher energy MOs by mixing only the MO pair of highest energy for a given symmetry classification, accepting as adequate representations those lower energy orbitals produced directly by angular variations of the higher symmetry structure. It is necessary to mix the highest energy pair only if the two MOs differ in the kinds of AOs of which they are composed. An important result of MO mixing is an added energy lowering or stabilization of the lower energy orbital and an energy destabilization of the higher orbital.

As the AO basis set for AB$_6$ we have chosen the single s and three p valence AOs of the central atom A and only one AO from each ligand B suitable for the formation of a σ-type bond to the central atom. The ligand AO might be a p orbital or some type of hybrid orbital pointing directly toward the central atom. For representational convenience, however, we depict the ligand orbitals as s AOs in all the accompanying diagrams. For AB$_6$ the ten AO basis set can be used to form ten MOs.
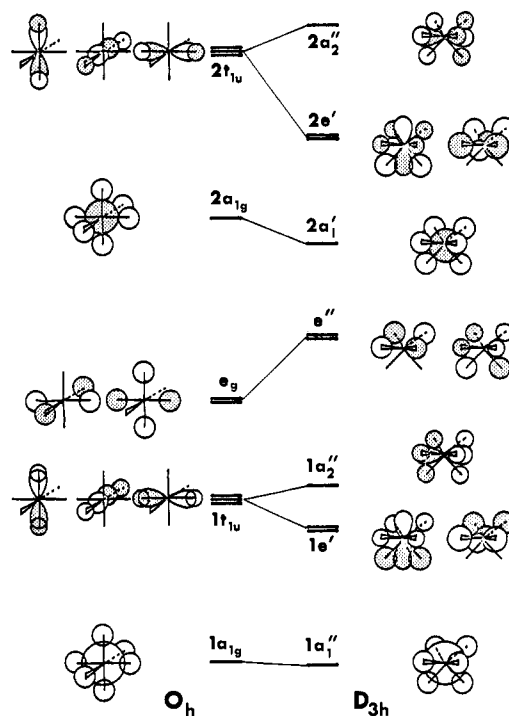

Figure 1. MO correlations for octahedral (O_h) and trigonal prismatic (D_{3h}) structures for AB$_6$ complexes.

The valence electrons are counted by including all of the electrons in the valence s and p AOs of the neutral central atom plus one electron from each halogen ligand (none from oxygen ligands) plus one electron for each negative charge on the complex as a whole (subtract positive charges).

Shapes of the AB$_6$ Series

Tables I and II list the known AB$_6$ halides of main groups 3 through 0 of the periodic table. Table I contains complexes with 12 valence electrons and Table II lists those with 14 valence electrons. Several 13-electron AB$_6$ radicals are also known. Examples are ClF$_6$,[7] BrF$_6$,[8] SF$_6^-$, and XeF$_6^+$. Although SbCl$_6^{2-}$ and SbBr$_6^{2-}$ have been reported,[9] the best evidence[10] indicates that these are not radical anions but rather mixed valence compounds containing SbX$_6^-$ and SbX$_6^{3-}$. Oxides with 12 valence electrons are SbO$_6^{7-}$,[11] TeO$_6^{6-}$,[12] IO$_6^{5-}$,[11] and XeO$_6^{4-}$.[13] They seem to follow the same scheme as the more numerous halides.

All AB$_6$ complexes for which structures have been determined are octahedral or nearly so. The octahedron (O_h) can be converted into a trigonal prism (D_{3h}) by the rotation of one

$$O_h \quad \text{—} \quad \longrightarrow \quad \text{—} \quad D_{3h}$$
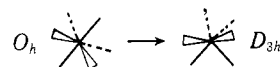
end of the structure by 60° relative to the other, assuming that A–B bond distances remain constant. This internal rotation is related to that connecting staggered and eclipsed ethane, a relationship pointed out by Hoffmann and co-workers.[3] The particular orientation of structures emphasizes the comparison with the internal rotation in ethane.

Figure 1 is a correlation diagram for the rotation from the octahedral or staggered structure to the trigonal prismatic or eclipsed conformation. This picture also contains an AO composition diagram for each MO. We chose the orientations of structures in Figure 1 for the ease of conceptual construction of the MOs. Symmetry requires that the O_h group contains doubly or triply degenerate orbitals. The triply degenerate levels must involve the three individual p AOs of the central atom overlapping two of the six ligand orbitals. Because both

Table I. Known AB_6 Halides. 12 Valence Electrons[a]

Group 3	Group 4	Group 5	Group 6	Group 7	Group 0
AlF_6^{3-} (1.800)	SiF_6^{2-} (1.706)	PF_6^- (1.599)	SF_6 (1.564)	ClF_6^+	
		PCl_6^- (2.06)			
		PBr_6^-			
GaF_6^{3-} (1.808)	GeF_6^{2-} (1.77)	AsF_6^- (1.67)	SeF_6 (1.688)	BrF_6^+	
	$GeCl_6^{2-}$ (2.35)	$AsCl_6^-$			
InF_6^{3-} (2.04)	SnF_6^{2-} (1.97)	SbF_6^- (1.84)	TeF_6 (1.824)	IF_6^+	
$InCl_6^{3-}$	$SnCl_6^{2-}$ (2.42)	$SbCl_6^-$ (2.35)			
$InBr_6^{3-}$	$SnBr_6^{2-}$ (2.61)	$SbBr_6^-$ (2.55)			
	SnI_6^{2-} (2.85)				
TlF_6^{3-} (1.96)	PbF_6^{2-} (2.15)	BiF_6^-			
$TlCl_6^{3-}$ (2.49)	$PbCl_6^{2-}$ (2.50)				
$TlBr_6^{3-}$ (2.59)					

[a] The numbers in parentheses are A–B bond distances in Å.

Table II. Known AB_6 Halides. 14 Valence Electrons[a]

Group 3	Group 4	Group 5	Group 6	Group 7	Group 0
		PCl_6^{3-}		ClF_6^-	
				BrF_6^-	
		$AsCl_6^{3-}$	$SeCl_6^{2-}$ (2.40)		
			$SeBr_6^{2-}$ (2.54)		
			SeI_6^{2-}		
		SbF_6^{3-}	TeF_6^{2-}	IF_6^-	XeF_6 (1.890)
		$SbCl_6^{3-}$ (2.652)	$TeCl_6^{2-}$ (2.541)		
	$SnBr_6^{4-}$	$SbBr_6^{3-}$ (2.799)	$TeBr_6^{2-}$ (2.70)		
	SnI_6^{4-}	SbI_6^{3-}	TeI_6^{2-} (2.90)		
	PbF_6^{4-}	BiF_6^{3-}			
	$PbCl_6^{4-}$ (2.93)	$BiCl_6^{3-}$ (2.66)	$PoCl_6^{2-}$ (2.54)		
	$PbBr_6^{4-}$ (3.12)	$BiBr_6^{3-}$ (2.840)	$PoBr_6^{2-}$ (2.64)		
	PbI_6^{4-}	BiI_6^{3-}	PoI_6^{2-} (2.82)		

[a] The numbers in parentheses are A–B bond distances in Å.
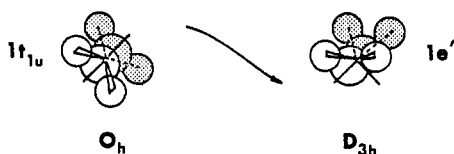

Figure 2. The energy of $1e'$ (D_{3h}) is lower than that of $1t_{1u}$ because in-phase ligand AOs are closer together.

in-phase and out-of-phase overlap combinations are possible there are two sets of the triply degenerate (t_{1u}) orbitals or a total of six MOs. Furthermore, there are two completely symmetric MOs (a_{1g}) made by in-phase or out-of-phase combinations of the central atom s orbital and the ligand AOs. The two remaining octahedral MOs must be the doubly degenerate e_g pair, represented below as a and b. That these two MOs have the same energy is obvious from their AO composition diagrams. For degenerate orbitals it is possible to draw an infinite number of alternative but equivalent AO composition diagrams. We chose to include a and b in Figure 1 for convenience only. In other circumstances it will be convenient to choose other representations.
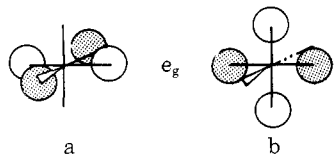
The e_g MOs are nonbonding. In our model they contain no AO contributions from the central atom, although they do have the symmetry of d AOs and had we included central atom d orbitals in our basis set they would have appeared in e_g. The ligand AOs in e_g are out of phase with their cis neighbors.

The energy ordering of the O_h energy levels is straightforward. At lowest energy is the bonding $1a_{1g}$ orbital and above that the bonding $1t_{1u}$. The nonbonding e_g orbitals are at intermediate energy and above them are the antibonding $2a_{1g}$ and the antibonding $2t_{1u}$. The order and spacing of the energy levels in Figure 1 are those obtained from extended Hückel[5] calculations for model AH_6 systems.

Consider the rotation of AB_6 from staggered or octahedral to eclipsed or trigonal prismatic. The eclipsed a_1' orbitals should have lower energy than their staggered relatives a_{1g} because the ligand orbitals can overlap each other better in the eclipsed conformation in which they are closer together. In the staggered conformation the ligands are as far apart as possible. The bonding and nodeless $1a_{1g}$ and $1a_1'$ MOs have very nearly equal energies but the higher energy antibonding set shows the predicted trend $a_{1g} > a_1'$. The t_{1u} orbitals split into an e' pair and a_2''. Figure 2, containing only one member of the $1t_{1u}$–$1e'$ orbitals, shows why the energy decreases from $1t_{1u}$ to $1e'$. In the rotation we keep the three ligands at the left-hand side of the O_h structure in Figure 2 fixed and we rotate the three right-hand ligands around the horizontal axis. Imagine the ligand on the nodal surface in the O_h picture rotating back and away from the nodal surface that eliminates its AO from the O_h MO and into a position in D_{3h} where the ligand AO can overlap in phase with the rear lobe of the central atom p AO. The ligand that was to the rear in O_h rotates down and to the nodal surface where its AO vanishes in D_{3h}. The third rotating ligand, the one overlapping the front lobe of the central atom p in O_h, moves up a bit with no change in phase. The rotation moves in-phase ligand AOs closer together to increase overlap and lower the MO energy. Rotation raises the energy of the component of $1t_{1u}$ that becomes $1a_2''$. Figure 3 explains why. Out-of-phase ligand AOs are closer together in $1a_2''$ than they are in $1t_{1u}$. This energy increase should be small for at least two
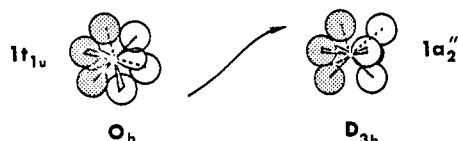
Figure 3. The energy of $1a_2''$ (D_{3h}) increases relative to $1t_{1u}$ (O_h) because ligand AOs on opposite sides of the nodal surface are closer together.

Figure 4. Out-of-phase ligand AOs are closer together in e'' (D_{3h}) than in e_g (O_h).

reasons: (1) The ligands are not particularly close to each other; i.e., they are not bound to each other. (2) Although the end–end ligands of one set move closer together, those of another set move farther apart. Therefore, the energy increase of $1a_1''$ above $1t_{1u}$ is considerably smaller than the energy lowering of e' below $1t_{1u}$ and the extended Hückel results support the qualitative reasoning. Furthermore, since $1a_{2''} > 1t_{1u}$ and $1e' < 1t_{1u}$, we can see that $1a_2'' > 1e'$ for the eclipsed or trigonal prismatic energy levels. Next, look at the energy increase of the octahedral or staggered e_g levels as they become the e'' levels of the trigonal prism or eclipsed conformation. Figure 4 shows the details. The out-of-phase overlaps increase between ligands at opposite ends of the rotational axis producing an energy increase. These MOs are double noded and the coefficients of the ligand AOs are large; therefore, the resulting energy changes occurring on rotation are large compared to those for $1a_2''$, $1e'$, or $1t_{1u}$ sets of lower energy.

Consider the correlation diagram of Figure 1 as a whole. A 12-electron molecule such as SF_6 should be octahedral (staggered) because of the greater stability of the highest occupied orbitals e_g (O_h) relative to e'' (D_{3h}). The 12-electron AB_6 complexes are structurally rigid, as is the 12-electron A_2H_6 analogue, diborane.[14] Although a ten-electron complex would not have a closed shell of electrons in either conformation, we expect that the octahedral configuration would still be preferred.[15] An eight-electron complex such as the hypothetical BeF_6 should be trigonal prismatic rather than octahedral. XeO_6 is another candidate for the trigonal prismatic structure. XeO_6^{4-} is known and octahedral. The electron affinity of the neutral XeO_6 might be too high to allow it to exist because of the empty e_g-e'' MOs. Pierce and Porter[16] claim to have observed two isomers of $BF_2H_4^+$ (eight electrons) in low-temperature ion–molecule reaction experiments in a BF_3-H_2 system. They picture one of the isomers as possibly involving four-coordinate boron with two of those coordinating bonds composed of H_2 units bound to the boron through three-center bonds. We would prefer to describe this structure as having a six-coordinate boron, although three-center B-H_2 units are also appropriate. We predict that a six-coordinate $BF_2H_4^+$ ion would be trigonal prismatic rather than octahedral.

Easterfield and Linnett[17] have done floating spherical Gaussian calculations for LiH_6^+ (six valence electrons) and related systems. They speculate that LiH_6^+ might be weakly bound and they suggest the kind of experiments in which it might be observed.[18] If the complex has a central atom, lithium is the logical choice and our model predicts that LiH_6^+ would be trigonal prismatic (D_{3h}) rather than octahedral (O_h). Hiraoka and Kebarle[19] think that the six-electron ion H_7^+ has a structure that can be described as an H_3^+ ion with two H_2 units attached at two corners of the H_3^+ triangle and perpendicular to the H_3^+ plane. In other words, H_7^+ does not have an atom at the center of the structure. A centrosymmetric
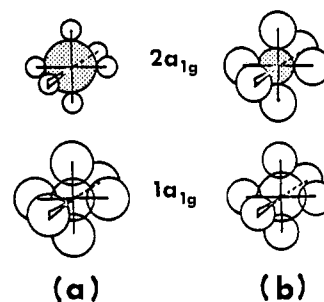

Figure 5. (a) Central atoms AO energy is far above that of ligand AOs. (b) Ligand and central atom AOs are close in energy.

structure such as D_{3h} requires a p AO on the central atom to make the occupied $1e'$ MOs bonding. The hydrogen 2p is high in energy above the 1s and therefore not likely to contribute to the $1e'$ MOs. On the other hand, the vacant 2p AOs of lithium are quite close to the 2s and, hence, much more likely to mix into the e' pair and make them bonding.

The 14-valence-electron complex, XeF_6 and IF_6^- are examples, would be isoelectronic with ethane and would be staggered (octahedral) rather than eclipsed (trigonal prismatic) for the same reasons that ethane is staggered: the antibonding dominant nature of the e_g, e'' orbitals, which lie below the highest occupied $2a_{1g}$-$2a_1'$ system.[20]

The highest occupied MO in the 14-electron AB_6 system is the antibonding $2a_{1g}$ orbital. Although this orbital is completely symmetric with respect to all symmetry operations of the O_h group, this does not mean that the orbital is at a relative energy minimum with respect to angular variations. In fact, just the opposite is true; octahedral geometry represents an energy maximum for a_{1g} orbitals because the in-phase overlapping ligand orbitals are as far apart as they can possibly be. Any angular change would bring two or more AOs closer together, increasing their overlaps and stabilizing the energy of the distorted MO. This must represent the driving force for distortions from pure octahedral symmetry. Bartell and Gavin[21,22] have suggested several such distortions to describe the fluxional behavior of XeF_6. The experimental structural data for XeF_6 have recently been reexamined by Pitzer and Bernstein.[23] Although XeF_6 easily distorts, isoelectronic species such as $TeCl_6^{2-}$, $TeBr_6^{2-}$, and $SbBr_6^{3-}$ seem to have regular octahedral structures. Our qualitative MO model can account for this trend. Two a_{1g} MOs can be made from the in-phase and out-of-phase interactions of the central atom s AO with the six ligand AOs. In a complex such as BiF_6^{3-} one expects the ligand AO energies to lie at low energy compared to that of the s AO on the central atom. If the energy of the central atom s orbital is high relative to that of the ligand AOs (meaning lower electronegativity for the central atom compared to the ligands), then the lower energy $1a_{1g}$ MO should be composed largely of ligand AOs while the $2a_{1g}$ MO should be mostly the central atom s AO with only small contributions from ligand AOs. If ligand AO coefficients are small in such a $2a_{1g}$ MO, a distortion from octahedral geometry will produce only a small energy lowering. See Figure 5(a). However, if the central atom–ligand AO energy gap is small, the ligand contributions to $2a_{1g}$ will be significant and a distortion from octahedral geometry will yield a large energy lowering. XeF_6 and Figure 5(b) serve to illustrate this situation. Therefore, the trend should be an increased tendency to distortion from octahedral symmetry as the energy difference between central atom s and ligand AOs decreases. This is just what is observed.

Formation of AB_6

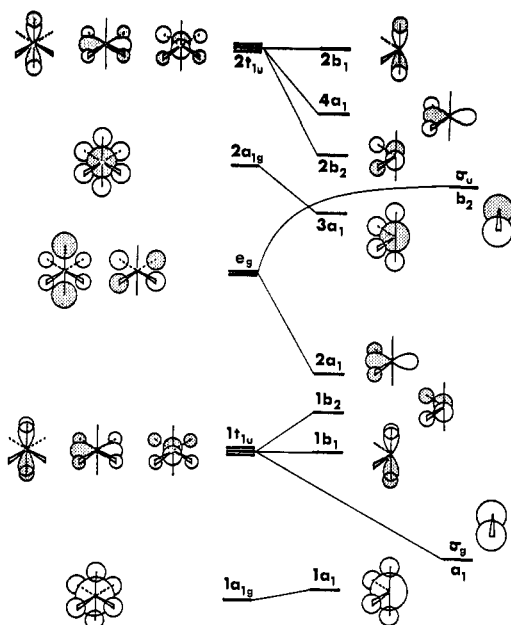The hexafluorides of sulfur, selenium, and tellurium are ordinarily prepared by burning these elements in fluorine.[24]

Figure 6. MO correlations for the dissociation of octahedral AB_6 into AB_4 and B_2.

By carefully controlling the conditions (0 °C or less, dilute fluorine) these reactions can be made to produce only the tetrafluorides.[25] SF_5Cl can be prepared by the direct reaction of SF_4 and ClF at 350 °C and 5 atm.[26] The same product can be formed much more readily and under milder conditions if SF_4 and CsF are first combined to form the adduct $Cs^+SF_5^-$ which is then reacted with ClF, forming SF_5Cl and regenerating CsF.[27] It is clear that the addition of the third halogen diatomic to the tetrafluorides is more difficult than the addition of the first two. To study this we look at the correlation diagram (Figure 6) for the reverse process:

$$AB_6 \rightarrow AB_4 + B_2$$

We assume a C_{2v} structure for the AB_4 product because it corresponds to the known geometry of the tetrafluorides of sulfur, selenium, and tellurium.

In constructing Figure 6 we have kept the angle between the two equatorial ligands of AB_4 fixed at 90° for simplicity. The orbitals in Figure 6 are classified according to the symmetry of the dissociation process, C_{2v}. The bonding MO of the product B_2 (a_1 or σ_g) is assumed to have an energy comparable to that of the nodeless $1a_1$ MO of AB_4 and below that of the group of AB_4 orbitals that are related in AO composition to the $1t_{1u}$ of AB_6. We have placed the antibonding MO (b_2 or σ_u) of the B_2 product below the antibonding $2b_2$ MO of the AB_4 product, but the order of these two MOs that have the same symmetry under the C_{2v} point group might conceivably be reversed depending on the particular system considered. With either ordering of these antibonding b_2 levels, the dissociation of 12-electron AB_6 complexes is symmetry forbidden[28] because electrons would flow from the e_g orbital of reactant AB_6 into either the σ_u (b_2) MO of B_2 as shown in Figure 6 or the $2b_2$ MO of AB_4, leaving $3a_1$ (AB_4) vacant at lower energy. If the order of antibonding b_2 levels of products is that shown in Figure 6, then the dissociation of 14-electron AB_6 complexes is also forbidden. Empirical evidence indicates that this is the case. The 14-electron complexes are synthesized by the addition of F^- to AB_5 rather than by direct addition of a diatomic halogen molecule to AB_4. Similar correlation diagrams show that dissociations of AB_4 into $AB_2 + B_2$ and AB_2 into $A + B_2$ are symmetry allowed.

$PbCl_6^{2-}$	2.50	$SbCl_6^-$	2.35	$SbBr_6^-$	2.55
$PbCl_6^{4-}$	2.93	$SbCl_6^{3-}$	2.65	$SbBr_6^{3-}$	2.80

Bond Lengths, Bond Strengths, and Relative Stabilities

Several isoatomic AB_6 pairs are known, the members of which are composed of the same ligand and central atom but for which the oxidation state of the central atom differs by 2. The member with the higher oxidation state contains 12 valence electrons and the one with the lower oxidation state has 14. Table III contains the pairs for which the A–B bond lengths are known for both members of the pair. In molecular orbital terms the difference between the members of an isoatomic pair is an electron pair occupying the antibonding $2a_{1g}$ MO of the 14-electron ion while $2a_{1g}$ is empty in the 12-electron member. An electron pair added to an antibonding MO should have the effect of weakening or lengthening the A–B bond and the data in Table III follow this rule. Other known isoatomic pairs include ClF_6^+, ClF_6^-; BrF_6^+, BrF_6^-; IF_6^+, IF_6^-; and PbF_6^{2-}, PbF_6^{4-}. We predict the member with the lower central atom oxidation state to have a considerably longer A–B bond length. Another measure of bond strengths is the symmetric stretching frequency ν_1 (a_{1g}) which is observed in the Raman spectrum. Again, the spectral data support our model: $PbCl_6^{2-}$ (ν_1 281 cm^{-1}),[29] $PbCl_6^{4-}$ (202);[30] $SbCl_6^-$ (329),[29] $SbCl_6^{3-}$ (267).[30] In each case the 14-electron ion has the lower stretching frequency. This discussion suggests that when comparing different classes of molecules in which the MOs are filled by electrons to different levels, there is no reason to expect bond distances between different pairs of the same kinds of atoms to be equal as required by the simple notion of the additivity of covalent radii. Where the additivity of radii works, it must be because comparable MO systems are occupied by electrons to the same level.

The highest occupied MO in 12-electron AB_6 molecules and ions is the doubly degenerate nonbonding e_g pair. The energies of these MOs are determined in part by the energy of the AOs of the component ligands. For example, if the ligand is fluorine then the e_g orbitals would have lower energy than if the ligand is iodine. If the stability of the complex is related to the stability of the highest occupied MO, then we would expect to see more fluorides than iodides among the 12-electron AB_6 complexes. A glance at Table I reveals that this is true. If a 12-electron AB_6 complex is known, its fluoride is known, chlorides, bromides, and iodides being less common in that order. Another factor that determines the energy of the e_g orbitals is the size of the central atom. Although central atom AOs do not enter e_g in our model, they do determine how far apart the ligand AOs are through participation in the bonding MOs at lower energy. Larger central atoms will separate the out-of-phase overlapping ligand AOs of e_g and, thereby, lower the orbital energy. This explains why chlorides, bromides, and iodides are more common for the complexes with larger central atoms, such as those at the bottoms of groups 4 and 5. The reduction of out-of-phase overlaps among ligand AOs in e_g by a large central atom or small ligands is the MO equivalent of traditional valence theory arguments based on steric repulsion which can also be used to explain these trends.

For the 14-electron AB_6 complexes iodides and bromides are much more likely than among the 12-electron series. Notice the pattern in Table II. Aynsley and Hetherington[31] have noted the trend of decreasing stability of tellurium halides TeX_6^{2-}: iodide > bromide > chloride > fluoride. Ahrland and Grenthe[32] show the same order for the bismuth(III) halides BiX_6^{3-}. It is clear that this stability trend, just the opposite of that for the 12-electron complexes, cannot be explained by simple ligand repulsion arguments. The difference between

the two series of complexes is that $2a_{1g}$ is occupied in the 14-electron cases but empty in the 12-electron complexes. For a given central atom, larger ligands would increase the ligand–ligand AO overlap, thereby stabilizing the energy of the MO. The in-phase ligand–ligand AO overlaps in $2a_{1g}$ are not large but there are 12 pairs of them. Exceptions occur if the central atom is xenon or a halogen. No chlorides, bromides, or iodides of halogen central atoms have been prepared in the 14-electron AB_6 series. Ligands must be more electronegative than the central atom to which they are bound because MO nodes run through or near the central atom, pushing electron density away from the central atom and toward the ligands. Recall that the energy of the e_g (O_h) orbitals is largely determined by the ligand AO energies. Placing the more electronegative element at the center and using the less electronegative element as ligands would increase the e_g energy.[33] For xenon and halogen central atoms, only fluorine is electronegative enough to serve as a ligand.

Other Models of Electronic Structure

Besides the reports of Urch[4] and of Hoffmann, Howell, and Rossi[3] there are several other important papers that bear on this work. The octahedral geometry of AB_6 complexes has long been explained by assuming octahedral d^2sp^3 hybrid orbitals on the central atom. Molecular orbital theory requires no assumptions about central atom hybridization. According to the valence shell electron pair repulsion (VSEPR) model of Gillespie and Nyholm[34] ligands and lone pairs occupy angular positions in which the repulsions among bonding pairs and unshared pairs of valence electrons are minimized. This easily accounts for the octahedral structure of the 12-electron complexes and for distortions from octahedral geometry of the 14-electron complexes in which such distortions have been observed. Not all 14-electron complexes are distorted, however. Gillespie[35] uses the VSEPR model to explain why XeF_6 distorts while isoelectronic species such as $TeCl_6{}^{2-}$, $TeBr_6{}^{2-}$, and $SbBr_6{}^{3-}$ seem to have regular octahedral structures. The ligands in $TeBr_6{}^{2-}$, for example, touch each other with no room for distortions from octahedral symmetry. The smaller ligands in XeF_6 give room for possible distortion. Gillespie further reinforces his argument by pointing out that $TeCl_6{}^{2-}$, $TeBr_6{}^{2-}$, and $SbBr_6{}^{3-}$ all have central atom–ligand distances that are considerably longer than the sum of the covalent radii of the atoms involved. We feel that we have offered alternative, qualitative MO explanations for these observations.

Summary

We have expanded some of the rules of qualitative MO theory. From qualitative comparisons of MO energies of AB_6 complexes in octahedral (O_h) and trigonal prismatic (D_{3h}) structures the preference of 12- and 14-electron complexes for octahedral geometry can be understood. Hypothetical eight-electron complexes should be trigonal prismatic. In the 14-electron series the highest occupied orbital is the A–B antibonding $2a_{1g}$ MO which accounts for the fact that 14-electron complexes have longer A–B bonds than do comparable 12-electron complexes. The ease with which 14-electron complexes can be distorted from octahedral symmetry is related to the

relative sizes of central atom and ligand AO coefficients in $2a_{1g}$ (O_h) which are determined by differences in central atom and ligand AO energies. The $2a_{1g}$ MO accounts for differences in the stabilities of the 12- and 14-electron complexes. In the 12-electron series, ligand–ligand out-of-phase overlaps in the highest occupied orbitals e_g are stabilized by large central atoms and small ligands (F). Known 14-electron complexes usually prefer large ligands (I) which stabilize $2a_{1g}$ through in-phase ligand–ligand overlaps. We hope that this kind of guided speculation will lead to detailed quantum mechanical calculations and new experiments.

References and Notes

(1) (a) University of South Carolina; (b) University of Maryland, Baltimore County.
(2) B. M. Gimarc, *Acc. Chem. Res.*, **7**, 384 (1974).
(3) R. Hoffmann, J. M. Howell, and A. R. Rossi, *J. Am. Chem. Soc.*, **98**, 2484 (1976).
(4) D. S. Urch, *J. Chem. Soc.*, 5775 (1964).
(5) R. Hoffmann, *J. Chem. Phys.*, **39**, 1397 (1963).
(6) J. P. Lowe, *J. Am. Chem. Soc.*, **96**, 3759 (1974).
(7) K. Nishikida, F. Williams, G. Mamanotov, and N. Smyrl, *J. Am. Chem. Soc.*, **97**, 3526 (1975).
(8) K. Nishikida, F. Williams, G. Mamantov, and N. Smyrl, *J. Chem. Phys.*, **63**, 1693 (1975).
(9) L. E. Sutton, Ed., *Chem. Soc.*, *Spec. Publ.*, **No. 11** (1958); **No. 18** (1965).
(10) S. L. Lawton and R. A. Jacobson, *J. Am. Chem. Soc.*, **88**, 616 (1966); C. R. Hubbard and R. A. Jacobson, *Proc. Iowa Acad. Sci.*, **75**, 85 (1968).
(11) H. Siebert, *Z. Anorg. Allg. Chem.*, **301**, 161 (1959).
(12) L. Helmholz, *J. Am. Chem. Soc.*, **59**, 2036 (1937); Y. D. Feikema, *Acta Crystallogr.*, **14**, 315 (1961); **20**, 755 (1966); H. Siebert and G. Wieghardt, *Z. Naturforsch. B*, **27**, 1299 (1972).
(13) D. M. Gruen, "Noble-Gas Compounds", H. H. Hyman, Ed., University of Chicago, 1963, p 174; Y. K. Gusev, V. K. Isupov, and I. S. Kirin, *Russ. J. Inorg. Chem.*, **18**, 294 (1973).
(14) B. M. Gimarc, *J. Am. Chem. Soc.*, **95**, 1417 (1973).
(15) R. G. Pearson, *Chem. Phys. Lett.*, **10**, 31 (1971); J. F. Liebman and J. F. Vincent, *J. Am. Chem. Soc.*, **97**, 1373 (1975).
(16) R. C. Pierce and R. F. Porter, *Inorg. Chem.*, **14**, 1087 (1975).
(17) J. Easterfield and J. W. Linnett, *Chem. Commun.*, 64 (1970).
(18) R. Clampitt and D. K. Jefferies, *Nature (London)*, **226**, 141 (1970).
(19) K. Hiraoka and P. Kebarle, *J. Chem. Phys.*, **62**, 2267 (1975).
(20) J. P. Lowe, *J. Am. Chem. Soc.*, **92**, 3799 (1970); *Science*, **179**, 527 (1973).
(21) R. M. Gavin and L. S. Bartell, *J. Chem. Phys.*, **48**, 2460 (1968).
(22) L. S. Bartell and R. M. Gavin, *J. Chem. Phys.*, **48**, 2466 (1968).
(23) K. S. Pitzer and L. S. Bernstein, *J. Chem. Phys.*, **63**, 3849 (1975).
(24) B. Cohen and R. D. Peacock, *Adv. Fluorine Chem.*, **6**, 343 (1970).
(25) E. E. Aynsley, R. D. Peacock, and P. L. Robinson, *J. Chem. Soc.*, 1231 (1952); F. Brown and P. L. Robinson, *ibid.*, 3147 (1955).
(26) F. Nyman and H. L. Roberts, *J. Chem. Soc.*, 3180 (1962).
(27) C. W. Tullock, D. D. Coffman, and E. L. Muetterties, *J. Am. Chem. Soc.*, **86**, 357 (1964).
(28) R. Hoffmann and R. B. Woodward, *Acc. Chem. Res.*, 1, 17 (1968).
(29) P. Labonville, J. R. Ferraro, M. C. Wall, and L. J. Basile, *Coord. Chem., Rev.*, **7**, 257 (1972).
(30) T. Barrowcliffe, I. R. Beattie, P. Day, and K. Livingston, *J. Chem. Soc. A*, 1810 (1967).
(31) E. E. Aynsley and G. Hetherington, *J. Chem. Soc.*, 2802 (1953).
(32) S. Ahrland and L. Grenthe, *Acta Chem. Scand.*, 11, 1111 (1957).
(33) R. E. Rundle, *J. Am. Chem. Soc.*, **85**, 112 (1963).
(34) R. J. Gillespie and R. S. Nyholm, *Q. Rev., Chem. Soc.*, 11, 339 (1957); R. J. Gillespie, *J. Chem. Educ.*, **47**, 18 (1970).
(35) R. J. Gillespie, "Werner Centenial", *Adv. Chem. Ser.*, **No. 62**, 221 (1967).